Attosecond streaking of photoelectrons emitted from metal surfaces

Boyan Obreshkov
Institute for Nuclear Research and Nuclear Energy,
Bulgarian Academy of Sciences, Tsarigradsko chausseé 72, Sofia 1784, Bulgaria

We numerically investigate attosecond streaking time delays in the photoemission of valence and 2p core electrons of aluminum surface. We find that electron emission from the core level band is delayed by $\Delta\tau = 100$ attoseconds relative to the release of electrons from the valence band. We show that this relative time offset in electron emission is caused by the screening of the streaking laser field by conduction electrons.

PACS numbers:

arXiv:1411.4996v1 [quant-ph] 17 Nov 2014

I. INTRODUCTION

The progress in development of ultrashort laser pulses has allowed time-resolved study of photoemission on atomic time scale. In attosecond time-resolved measurements of photoelectron emission from metal surfaces, attosecond ($10^{-18}s$) extreme ultraviolet (XUV) light pulse is used to ionize electrons from either bound core levels or delocalized conduction-band states. The released electrons move toward the surface, where they are exposed to an intense few-cycle infrared (IR) laser pulse at the moment of their escape from the surface. The electric field of the IR pulse modulates the kinetic energy of the electrons depending on their release time from the crystal. Although valence and core electrons are ionized at the same time, it was experimentally found that they emerge from the surface at different times, therefore their measured kinetic energies showed a small relative time shift $\Delta\tau$. In this experiment [1], the emission of 4f core electrons of tungsten was found to be delayed relative to the valence band by 110 ± 70 attoseconds.

This small time difference has been explained with several different theoretical models. Classical transport simulations [2] interpreted this time delay as the difference in the average travel times of electrons emerging from delocalized valence-band and tightly bound core states to the surface of the crystal. In contrast, quantum mechanical calculations suggest that the observed time delay is due to the different degree of spatial localization of initial state wave functions [3, 4].

Time resolved photoionization of (free-electron-like) Mg(0001) surfaces [5] found no relative time delay in the streaked electron emission from localized 2p core and valence band states of Mg. The authors suggested that transport-related contributions to attosecond time delays can be explained in terms of quotient of group velocities and mean free paths of photoelectrons during their propagation inside the bulk, regardless of the different degree of localization of initial state wave-functions.

By solving the time-dependent Schrodinger equation with realistic 1D model potentials describing the electron-metal interactions, Ref. [6] explained this vanishing delay as a result of dominant electron emission from the bulk valence bands of Mg via resonant interband transitions. The sensitivity of relative time delays to the time-dependent response of the substrate electronic structure was further investigated and elaborated in Ref.[7], in particular the experimental observation in Ref.[5] was reproduced provided the energy-dependence of the photoelectron mean free path and the screening of the IR field at the surface are properly described.

Common to these model calculations is the description of the electronic structure by 1D model potentials, thereby assuming uniform motion of the photoelectrons parallel to the surface. Furthermore the screening of IR field by conduction electrons was described phenomenologically in terms of classical skin depth. The purpose of this paper is not to refine the theoretical description, but to investigate to what extent screening of the IR field by conduction electrons affects relative time delays in photoemission. The paper is organized as follows, In Sec.2 we present our theoretical model, Sec.3 discusses numerical results on streaking time delays in the photoemission from free-electron jellium Al surface and Sec.4 contains our main conclusions.

II. THEORETICAL MODEL

In one electron approximation, the time-dependent Hamiltonian for a free-electron like metal surface interacting with electromagnetic XUV and IR fields can be written as

$$H(t) = H_0 + H_{\rm int}(t) \tag{1}$$

and $H_0 = T + V_{\rm eff}$ is the field-free Hamiltonian given in terms of an effective one-electron potential. In velocity gauge the interaction Hamiltonian is

$$H_{\rm int}(t) = V_X(t) + V_{\rm IR}(t) = A_X(t-\tau)p_z + \frac{1}{2}(A_z(z,t)p_z + p_z A_z(z,t) + A_z^2(z,t)) \tag{2}$$

where $p_z = -i\partial_z$ and τ is the time delay between the IR and XUV laser pulses. The temporal profile of the XUV pulse is modelled by a Gaussian function

$$A_X(t) \sim e^{-\ln(4)(t/\tau_X)^2} e^{-i\omega_X t}, \tag{3}$$

with a pulse duration $\tau_X = 432$ as, central frequency $\omega_X = 118$ eV. The IR streaking field is approximated by its classical form

$$A_z(z,t) = \theta(z)A(t), \tag{4}$$

where θ is the Heaviside step function, Gaussian envelope of the IR laser pulse is assumed

$$A(t) = A_0 \sin(\omega_L t) e^{-\ln(4)(t/\tau_L)^2} \tag{5}$$

with pulse duration $\tau_L = 200$ a.u. and driving frequency $\omega_L = 1.5$ eV, the amplitude A_0 is chosen such that the peak intensity of the IR pulse is $I \approx 10^{12}\mathrm{W/cm}^2$. The approximation of Eq.(4) relies on the assumption of abrupt change of screening properties at the metal-vacuum interface, which is reasonable since the laser frequency ω_L is well below the bulk plasmon excitation threshold. Though it is known that the detailed spatial behavior of the electromagnetic potential within a few angstrom of the metal surface is relevant [8], our independent investigation based on the random phase approximation shows that the use of non-analytic vector potential is well justified for a high density substrate such as Al.

Treating the interaction with the XUV pulse as a perturbation, the time evolution operator is

$$U(t,t_0) = U_1(t,t_0) - i\int_{t_0}^{t} dt' U_1(t,t') V_X(t') U_1(t',t_0), \tag{6}$$

where U_1 describes the propagation of the electron in the screened IR field, which is formally given by the chronological Dyson's exponent

$$U_1(t,t_0) = T\exp\left(-i\int_{t_0}^{t} H_1(t)dt\right), \tag{7}$$

where $H_1(t) = H_0 + V_{\rm IR}(t)$. The photo-ionization amplitude from an initial target state $|i\rangle$ to a final continuum state $|f\rangle$ with kinetic energy E_f

$$T_{fi} = \langle f|U_1(+\infty,-\infty)|i\rangle - i\int dt \langle f|U_1(+\infty,t)V_X(t)U_1(t,-\infty)|i\rangle \tag{8}$$

includes a background contribution describing multi-photon ionization process driven by the IR field (first term), and a resonant contribution associated with the emission of electrons into the laser-dressed continuum of final states (second term). We neglect the first term and approximate the transition amplitude by

$$T_{fi}(\tau) \approx -i\int_{-\infty}^{\infty} dt A_X(t) p_{fi}(t), \tag{9}$$

where $p_{fi}(t) = \langle \phi_f(t)|p_z|\phi_i(t)\rangle$ is the off-diagonal matrix element of the momentum, the streaked photoemission probability is given by the incoherent sum over initially occupied substrate states

$$P_f(\tau) = P(E_f,\tau) = \sum_i n_i |T_{fi}(\tau)|^2. \tag{10}$$

After spectrally averaging the streaking traces in Eq.(10), we obtain time delays in photoemission from the relative displacement of the kinetic energy centroids $\langle E_f(\tau)\rangle = \int dE_f E_f P(E_f,\tau)/\int dE_f P(E_f,\tau)$. To specify the final state wave-function, we numerically solve the Schrödinger equation in momentum space by a wave-packet propagation method (cf. Appendix)

$$i\partial_t \phi_f(p,t) = \frac{1}{2}p^2\phi_f(p,t) + \frac{i}{2}A(t)\int_C \frac{dp'}{2\pi}\frac{p+p'+A(t)}{p-p'+i\eta}\phi_f(p',t) \tag{11}$$

where $\eta > 0$ is a positive infinitesimal and the contour C is along the real axis. We model the initial state wave-functions of weakly bound valence electrons by jellium wave-functions with binding energies $\varepsilon_k = (k^2 - k_F^2)/2$, where k_F is the Fermi momentum

$$\phi_k(p,t) = e^{-i\varepsilon_k t}\left(\frac{1}{p-k+i0} + \frac{e^{2i\eta_k}}{p+k+i0} - 2\frac{e^{i\eta_k}\cos\eta_k}{p-i\kappa}\right), \tag{12}$$

$\eta_k = -\arctan(\kappa/k)$ is a reflection phase, $\kappa = \sqrt{2(W-\varepsilon_k)} > 0$ is the surface barrier penetration coefficient and $W = 4$ eV is the Al workfunction. We assume simple tight-binding approximation for the description of the initial 2p core-level wavefunctions

$$\phi_\theta(p,t) = e^{-i\varepsilon_{2p}t}\Delta_\theta(p)u_{2p}(p), \tag{13}$$

in terms of planar-averaged structure factor

$$\Delta_\theta(p) = \sum_{l=1}^{N_l}\sin(l\theta)e^{ipz_l}, \tag{14}$$

where $z_l = -(l-1/2)a_s$ labels the positions of the bulk atomic layers relative to the jellium edge ($z = 0$) of the surface and $a_s = 3.8$ is the interlayer spacing for the Al(100) surface. The phase parameter $\theta = ka_s$ changes in the first Brillouin zone $0 \le \theta \le \pi$. The atomic wavefunction $u_{2p}(p)$ is an eigenfunction of Yukawa-type screened Thomas-Fermi potential with binding energy $\varepsilon_{2p} = 72$ eV relative to the Fermi level ($\varepsilon_F = 0$).

III. NUMERICAL RESULTS AND DISCUSSION

The streaked photoemission spectra of valence and 2p core level bands of aluminum are shown in Fig.1. The spectrograms display the modulation of the photoelectron kinetic energy as a function of the IR-XUV time delay τ. The centroids of the streaked emission spectra follow the time variation of the IR field, as shown in Fig.2. Noticeably photoelectrons released from the 2p core level experience much weaker kinetic energy shifts by interacting with the IR field. More importantly the relative displacement of the streaking curves corresponds to a time delay of $\Delta\tau \approx 108$ as in the emission of 2p core electrons relative to the valence band. This time offset is in very good quantitative agreement with the experimental data in Ref.[1]. For comparison streaking curves for photoemission into a spatially uniform IR vector potential are also shown. In this case kinetic energy shifts of released valence and core electrons are strictly synchronized in time, i.e. there is no relative time delay in their emission. Since the time-dependent response of valence electrons to the screened vector potential causes their advanced emission relative to their emission in the unscreened vector potential, this comparison suggests that the time shift of 100 as is exclusively due to propagation effects of released electrons into the screened IR field, moreover in this case the initial state wave-functions $\phi_i(p)$ involved in the transition are unchanged.

To anlayze these results further, in Fig.3(a-d) we plot the time evolution of the Fourier coefficients $c(E_f, p_n, t)$ in the expansion of the photoelectron wave-function over plane-waves (cf. Appendix). Fig.3(a-b) compares the time development of the IR-field induced admixtures to the central momentum $p_f = 2.8$, Fig.(a), and $p_f = 1.8$ in Fig.(b). Propagating backwards toward the remote past, the coupling to the IR field gradually builds-up the photoelectron wave-packets by adding up coherently contributions of nearby momentum eigenstates. The wave-packets are fully formed for large negative times $t \le -200$ (remote past), when the Fourier amplitudes change harmonically over time $c(E_f, p, t) = c(E_f, p)e^{-ip^2/2t}$. As this comparison suggests the build-up of the wave-packet is less efficient for electrons released into lower kinetic energy states. Fig.3(c) shows the time evolution of the central component $c(E_f, p_f, t)$ of the wave-packet, the mean-squared fluctuation of the carrier momentum $\sigma_p = \sqrt{\langle p^2\rangle - \langle p\rangle^2}$ is also shown in Fig.3(d). The momentum spread over nearby states leads to uncertainty $\sigma_p \le 0.01$ a.u., i.e. $\sigma_p \ll p_f$, so that the Fourier coefficients are only appreciable in a narrow range near the mean momentum p_f during the whole time evolution.

The time evolution of the modulus of the momentum-space wave-function for the lower kinetic energy state is shown in Fig.4(a-d). The wave packet is fully formed in the distant past ($t = -500$), when density of states is peaked at p_f and is structured by narrow sidebands equidistantly spaced by $\delta p = 0.03$ a.u. above and bellow p_f. The number of sidebands depends sensitively on the number of half-cycles of the driving pulse. When the time increases to $t = -150$, Fig.4(b) the sidebands are distorted and slightly overlap. At the peak intensity of the IR electric field ($t = 0$), Fig.4(c), the sideband structure is blurred showing relevance of transient effects in the electron dynamics. The change in the density of states causes reduction of the wave-packet for large positive times $t = 150$, Fig.4(d), which is because electrons emerge in the low-intensity tail of the IR pulse and can undergo only weak change of their momenta. In the

far future $t \to \infty$, the components of the wave-packet are projected out describing the final free-electron state with momentum p_f at the detector.

Fourier transforming these results to coordinate representation, snapshots of the streaked photoelectron density relative to the free electron density $\delta n(z,t) = |\psi(z,t)|^2 - 1$ are shown in Fig.5(a-d). If electrons were promoted into the laser dressed continuum during the remote past $t = -500$, Fig.5(a), the IR pulse has ceased and thus wave-packets are fully formed. Their charge density distributions display characteristic longwavelength spatial modulation inside the bulk (with a wavelength of about 20 nanometers) . The crests of the wave-packets move freely towards the surface following the classical path $z = -z_{in} + v_{in}t$ with mean velocity v_{in}, but lag behind by a distance $z_{in} > 0$ relative to the free-electron motion. The speeds of the electrons at the instant of ionization are $v_{in} = 2.801$ and $v_{in} = 1.799$ a.u., respectively. The space shift Δz between the crests corresponds to a relative time delay $t_0 = -z_{in}/v_{in}$, which is $t_0 \approx -1400$ as for the higher energy state, while for the lower energy one $t_0 \approx -1380$ as. If the uniform motion of the crests is extrapolated into the surface region $z = 0$, it would suggest that electrons released into lower kinetic energy states arrive at the surface slightly earlier by $\Delta\tau = 20$ as. However this classical estimation is inconsistent with the time shift of 100 as we obtain from the displacement of the streaking curves in Fig.2. The naive time definition based on the movement of the crest is too crude to account for the spreading and re-shaping of the wave-packets as electrons move towards the surface. The final speeds are $v_f = 2.830$ and $v_f = 1.801$, respectively, showing that the higher energy state is accelerated by the IR field $\Delta v = v_f - v_{in} = 0.03$ a.u., while electrons released into lower kinetic energy states experience negligible velocity shifts.

If electrons were ionized at a later time $t = -150$, Fig.5(b), the crests of the wave-packets have moved closer to the surface, the spatial profile of the bulk charge density modulation changes due to reshaping of the wave-packets. If electrons are ionized at the peak intensity of the IR pulse, Fig.5(c), the free-electron motion is strongly perturbed by the IR field causing sharp truncation of the charge densities at the jellium edge. Such rather abrupt variation of the density near the surface is because photoelectrons increment their momenta $p \to p + A(t)$ after passing into the radiation-filled half-space ($z > 0$). This can be formally expressed by the jump of the derivative of the wave-function at the jellium edge $z = 0$, i.e.

$$\frac{\partial\psi}{\partial z}(z = 0^+, t) - \frac{\partial\psi}{\partial z}(z = 0^-, t) = -iA(t)\psi(z = 0, t). \tag{15}$$

Though the ordinary derivative has a discontinuity at $z = 0$, the covariant derivative $[\partial_z + iA(z,t)]\psi(z,t)$ remains continuous across the metal-vacuum interface. The electron density converges to a spatially uniform distribution for large positive times $t = 150$ (far future), Fig.5(d), such that wave-packets are dissolved and reduce to a single plane wave state $|\psi(t \to \infty)\rangle \to |p_f\rangle$ describing the emitted electron.

To further analyze temporal changes of photoelectron distributions, it is more instructive to decompose the photoelectron wave-function according to

$$\psi(z,t) = a(t)e^{ip_f z} + \sum_{p_n \neq p_f} \sqrt{w_n}c(p_n,t)e^{ip_n z} = \psi_f(z,t) + \psi_{fluc}(z,t) \tag{16}$$

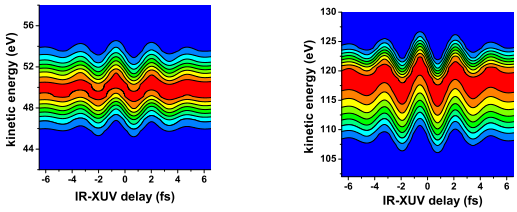

FIG. 1: Streaking spectrograms $P(E_f, \tau)$ of the valence band (a) and 2p core-level band (b) of an Al(100) surface as a function of the IR-XUV pulse delay τ and kinetic energy of released electrons into the screened IR field. Negative time delay ($\tau < 0$) corresponds to XUV preceding the IR pulse.

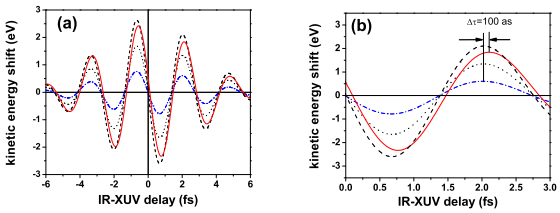

FIG. 2: Kinetic energy shifts for streaked photoemission from Al(100) surface. In Fig.(a) and Fig.(b) black dashed line gives result for the valence electron emission into the unscreened streaking field, solid red line - release of valence electrons into the screened IR field, black dotted line – emission of Al-2p core electrons into the unscreened potential and blue dashed-dotted line - release of Al-2p core electrons into the screened streaking field.

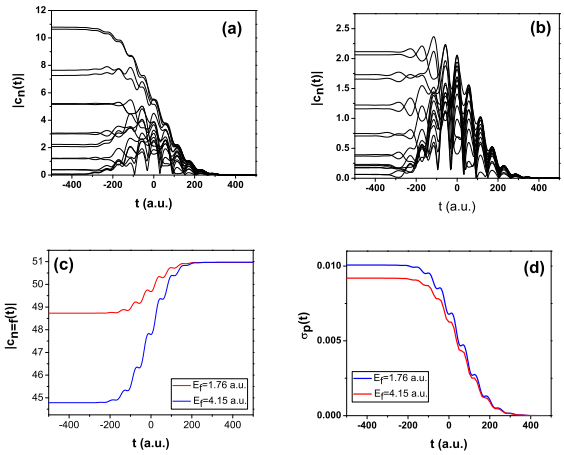

FIG. 3: Time evolution of the Fourier coefficients in the expansion of the wave-function over plane waves. In Fig. (a) the kinetic energy of the released electron is $E_f = 4.15$ a.u. and it is $E_f = 1.76$ a.u. in Fig. (b). For these two specific final kinetic energies Fig.(c) gives the time evolution of the central momentum components of the two wave packets. Fig.(d) gives the temporal variation of the mean squared fluctuation of the photoelectron momentum $\sigma_p = \sqrt{\langle p^2\rangle - \langle p\rangle^2}$.

where the first term is a renormalized plane-wave of the photoelectron with mean momentum p_f and the momentum spread over nearby states is represented by the fluctuating part of the wave-function ψ_{fluc}. In Fig.6(a-f) we plot the time-evolution of the fluctuating part of the charge density $n_{fluc}(z,t) = |\psi_{fluc}(z,t)|^2$ for electrons released into the screened IR field, for comparison the field-free time evolution is also shown. The field-free wave-packet is given by

$$\psi_0(z,t) = a_0(t \to -\infty)e^{ip_f z}e^{-ip_f^2/2t} + \sum_{p_n \neq p_f} \sqrt{w_n}c(p_n, t \to -\infty)e^{ip_n z}e^{-ip_n^2 t/2}. \quad (17)$$

Both ψ and ψ_0 satisfy the free Schrödinger equation inside the metal $z < 0$. As Fig.(6)(a) demonstrates, the wave-packet of the sideband momentum eigenstates is spatially localized and is represented by a normalized wave-function. Inside the metal, the free- and streaked- electron distributions display interference fringes that are slightly displaced on a sub-nanometer length scale. Both wave-packets are travelling in the direction of the positive z-axis (the vacuum half-space) at a constant speed. However unlike the freely moving wave-packet, the front-end of the streaked wave-packet is truncated inside vacuum, i.e. ψ_{fluc} has no propagating component in the radiation-filled half-space but

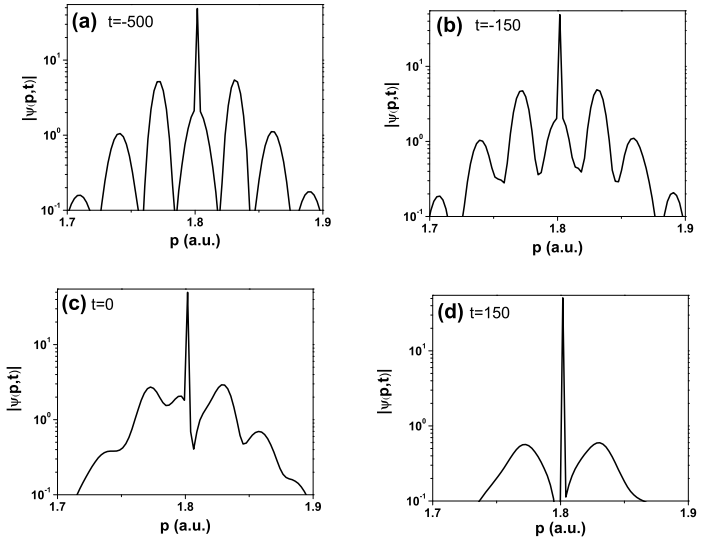

FIG. 4: Time evolution of the modulus of a laser-dressed wave-function $|\phi_f(p,t)|$ of a photoelectron released with kinetic energy $E_f = 1.8$ a.u.

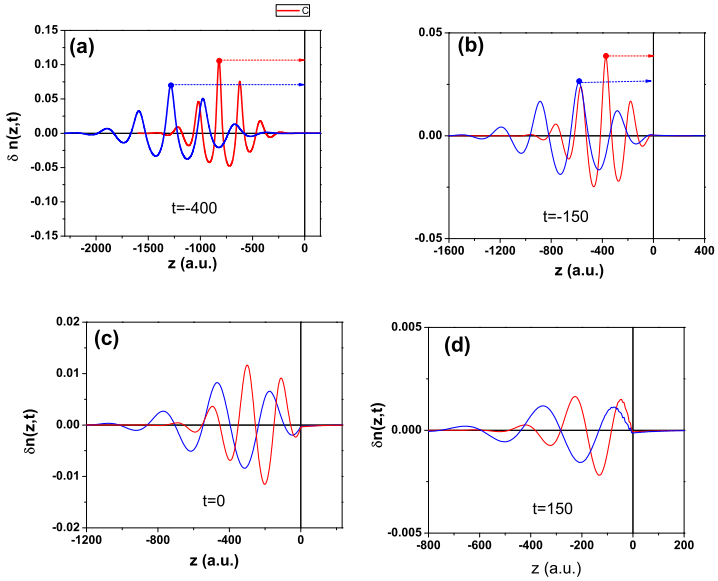

FIG. 5: Time evolution of the streaked photoelectron density $\delta n(z,t) = |\psi(z,t)|^2 - 1$ relative to the uniform free-electron density, here $\psi(z,t)$ is the (inverse) Fourier transformation of $\phi(p,t)$ and z is the coordinate normal to the surface. The metal occupies the half-space $z < 0$ and $z > 0$ designates the radiation filled vacuum half-space. The blue curves correspond to electrons released from the valence band and red curves to photoelectrons released from the 2p core-localized states.

only slowly decaying evanescent one. At the peak intensity of the IR pulse ($t = 0$), cf. Fig.(6)(b), the wave-packet is strongly distorted, the front-end part is truncated inside vacuum (relative to the free motion), the probability density remains localized at the metal-vacuum interface. Inside metal ($z < 0$), where the electric field of the IR pulse is fully screened, the back-end of the wave-packet is spatially shifted by $\Delta z = 0.5$ nm relative to the free motion. This space shift corresponds to relative time delay $\Delta\tau = \Delta z/v_f \approx 100$ as in the release of electrons into the streaking field. The

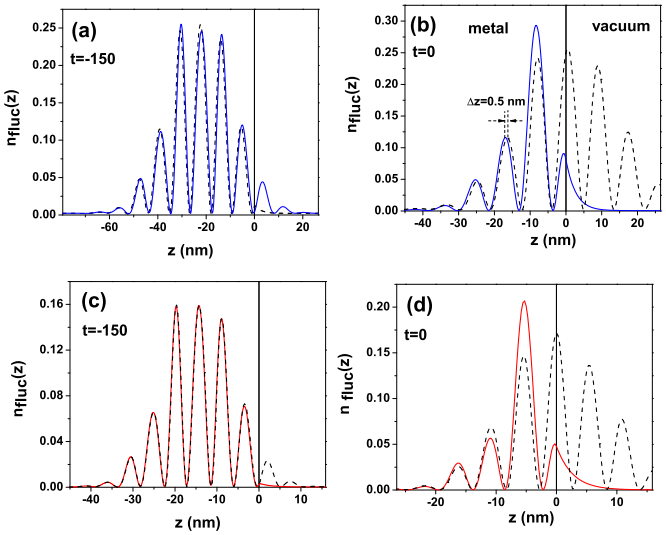

FIG. 6: Time evolution of the sideband structure of streaked photoelectron wave-packet. The dashed and solid lines in (a-d) give the field-free ($A = 0$) and field-dependent time evolutions, respectively. Fig.(a) and (b) give density distributions for photoelectrons released with kinetic energy $E_f = 4.15$ at times of ionization $t = -150$ and $t = 0$, respectively. Fig.(c) and (d) show the distributions of photoelectrons released with kinetic energy $E_f = 1.76$ at times of ionization $t = -150$ and $t = 0$, respectively. The distance to the surface is given in nanometers, the metal occupies the half-space with $z < 0$ and $z > 0$ is the radiation-filled half-space).

direction of the shift shows that photoelectrons move at a higher speed in the radiation filled half-space and are thus emitted in advance (relative to the free-electron motion). As this comparison demonstrates, the time shift we get in this way is in agreement with the timing information we get from the relative shift of the streaking traces in Fig.1. This confirms our observation that change in propagation of photoelectrons upon screening of the electromagnetic field by conduction electrons gives dominant contribution to the relative time delay in the photoemission.

Similar results are obtained for electrons released from the 2p-core level states of Al, Fig.(6)(c-d). The difference is that the relative phase shift inside the metal caused by the interaction with the IR field is vanishingly small, resulting in no noticeable relative time delay in the emission of core electrons (relative to the free motion).

IV. CONCLUSION

Based on wave-packet propagation study, we have investigated attosecond time delays in the photoemission from Al surfaces. We find that 2p core electrons are emitted with delay relative to the valence band by 100 attoseconds. We find that screening of the IR field is essential determinant for the calculation of the relative time delays in the emission. This relative time offset in the emission results from electron propagation effects (spreading and re-shaping of the wave-packets) in the screened electric field of the IR pulse. Though our numerical result does not include corrections to the streaking time shifts due to electron-electron and electron-ion collisions inside the bulk, we find the result is in very good quantitative agreement with the experiment. More detailed investigation of these effects is a subject to our follow-up paper. We also hope this work may become helpful in interpretation of experimental data on attosecond time-resolved photoemission from metal surfaces.

Appendix

The Schrödinger equation $i\partial_t\phi(t) = H(t)\phi(t)$ is discretized in momentum space using Gauss-Legendre mesh points p_n with weights w_n ([9])

$$i\partial_t c_n(t) = \sum_m H_{nm}(t)c_m(t), \tag{18}$$

and the definitions

$$c_n(t) = \sqrt{w_n}\phi_f(p_n, t), \tag{19}$$

where

$$H_{nm}(t) = \frac{1}{2\pi}\sqrt{w_n w_m}H(p_n, p_m, t), \tag{20}$$

is the matrix representation of the Hamiltonian. The Fourier transformation of the vector potential is

$$A(p,t) = \frac{iA(t)}{p - i\eta} \tag{21}$$

and η is a positive infinitesimal. The matrix representation of the Hamiltonian becomes

$$H_{nm}(t) = \frac{p_n^2}{2}\delta_{nm} + \sqrt{w_n w_m}\frac{i}{4\pi}A(t)\frac{p_n + p_m + A(t)}{p_n - p_m + i\eta}. \tag{22}$$

Taking the limit $\eta \to 0$, we obtain

$$i\partial_t c_n(t) = \varepsilon_n(t)c_n(t) + \sum_{m\neq n} V_{nm}(t)c_m(t) \tag{23}$$

with diagonal kinetic energies

$$\varepsilon_n(t) = \frac{1}{2}\left(p_n + \frac{1}{2}A(t)\right)^2 + \frac{1}{8}A^2(t) \tag{24}$$

and off-diagonal time-dependent couplings

$$V_{nm}(t) = \frac{i}{4\pi}\sqrt{w_n w_m}A(t)\frac{p_n + p_m + A(t)}{p_n - p_m}, \quad p_n \neq p_m \tag{25}$$

We propagate numerically the equations of motion with the Crank-Nicholson method for small equidistant time steps $\delta = 6$ as

$$\left(\mathbf{I} + i\frac{\delta}{2}\mathbf{H}(t)\right)\cdot\mathbf{c}(t-\delta) = \left(\mathbf{I} - i\frac{\delta}{2}\mathbf{H}(t)\right)\cdot\mathbf{c}(t), \tag{26}$$

subject to the final conditions $c_n(p_f) = \delta_{nf}/\sqrt{w_f}$ specified in the remote future $t \to \infty$. The off-diagonal matrix elements of the momentum are evaluated using these mesh points

$$p_{fi}(t) = e^{-i\varepsilon_i t}\sum_{n=1}^{N}\sqrt{w_n}c_n^*(t)p_n\phi_i(p_n) \tag{27}$$

For the strip $[p_f - 0.5, p_f + 0.5]$, convergence is reached when the number of basis states $N \geq 549$, here $p_f = \sqrt{2(E_f - W)}$ is the central photoelectron momentum.

Acknowledgements

The author thanks N. Minkov and A. Georgieva for providing a slot to give a talk on "Attosecond streaking of electrons from metal surfaces" at the 33rd International Workshop on Nuclear Theory IWNT33-2014.

---

[1] A. L. Cavalieri, N. Müller, Th. Uphues, V. S. Yakovlev, A. Baltuška, B. Horvath, B. Schmidt, L. Blümel, R. Holzwarth, S. Hendel, M. Drescher, U. Kleineberg, P. M. Echenique, R. Kienberger, F. Krausz, and U. Heinzmann, Nature (London) **449**, 1029 (2007).
[2] C. Lemell, B. Solleder, K. Tőkesi,, and J. Burgd¨orfer, Phys. Rev. A **79**, 062901 (2009).
[3] A. K. Kazansky and P. M. Echenique, Phys. Rev. Lett. **102**, 177401 (2009).
[4] C.-H. Zhang and U. Thumm, Phys. Rev. Lett. **102**, 123601 (2009).
[5] S. Neppl, R. Ernstorfer, E. M. Bothschafter, A. L. Cavalieri, D. Menzel, J. V. Barth, F. Krausz, R. Kienberger, and P. Feulner, Phys. Rev. Lett. **109**, 087401 (2012).
[6] A. G. Borisov, D. Sánchez-Portal, A. K. Kazansky, and P. M. Echenique, Phys. Rev. B **87**, 121110(R) (2013).
[7] Q. Liao and U. Thumm, Phys. Rev. Lett. **112**, 023602 (2014).
[8] P. J. Feibelman, Phys. Rev. B **12**, 1319 (1975).
[9] R. G. Littlejohn, M. Cargo, T. Carrington, Jr., K. A. Mitchell, B. Poirier, J. Chem. Phys. **116**, 8691 (2002).